forests

MDPI

Article

Genome-Wide Identification, Characterization, and Expression Profiling of the *UBP* Gene Family in *Prunus mume* Under Chilling and Freezing Stresses

Wenqing Zheng [1,*], Jinyu Fan [1], Jiakai Zhao [1], Yajing Duan [1], Jie Meng [1] and Xi Zhang [2,*]

[1] Department of Horticulture and Landscape, Taiyuan University, Taiyuan 030032, China
[2] National Key Laboratory of Forest Tree Genetics and Breeding, School of Biological Science and Technology, Beijing Forestry University, Beijing 100083, China
* Correspondence: zhengwenqing@bjfu.edu.cn (W.Z.); zhangxi@bjfu.edu.cn (X.Z.)

Abstract

The *UBP* gene family plays a key role in various physiological processes, including cell cycle regulation, DNA repair, and stress responses. *UBPs* have been identified and analyzed in several species, including *Moso Bamboo*, *Arabidopsis thaliana*, *Oryza sativa* L., and *Brachypodium distachyon*. However, the *UBP* family within *Prunus mume* Siebold & Zucc. remains unexplored. In this study, 30 *PmUBP*s were identified and characterized, all of which contained the UCH conserved domain. They were grouped into 16 subfamilies via evolutionary analysis, revealing similarities in genome structure and motif distribution. *PmUBP*s were distributed on seven chromosomes and three scaffolds. Gene duplication events, including tandem duplication and segmental duplication, promoted the expansion of *PmUBP*s. Collinear analysis demonstrated the close relationship between *P. armeniaca*, *P. persica*, *P. avium*, and *P. mume*. Transcriptome data revealed distinct relative expression trends in *PmUBP* genes across different tissues. Promoter cis-acting element analysis revealed an abundance of hormone-, light-, and stress-responsive elements across all genes. Transcriptome and reverse transcription quantitative PCR (RT-qPCR) analysis showed that *PmUBP2*, *PmUBP11*, *PmUBP13*, *PmUBP18*, *PmUBP22*, and *PmUBP26* exhibited relatively high expressions under low-temperature stress. This study provides a theoretical foundation for the role of *PmUBP* genes in response to low-temperature stress.

Keywords: *Prunus mume*; deubiquitinase; evolution; low-temperature; expression

1. Introduction

Protein ubiquitination is a post-translational regulatory mechanism in eukaryotes [1]. Numerous research advances have revealed the importance of this modification for many processes related to growth and development, including transcriptional regulation of functional genes, cell cycle regulation, repair of damaged plant cells, and responses to biotic and abiotic stresses [2–5]. The ubiquitination of proteins is a regulated reversible process that enables ubiquitin molecules to be reused. More specifically, ubiquitination is reversed in a reaction catalyzed by deubiquitinases, which help regulate the ubiquitination system, thereby controlling proteins' various physiological activities [6].

Deubiquitinase family members are divided into the following two major categories according to amino acid sequence similarities and protease functions: cysteine protease and metalloprotease [7,8]. Cysteine proteases have been further divided into the following four families according to the differences in their domains that interact with ubiquitin

Check for updates

Academic Editor: Chenghao Li

Received: 2 June 2026
Revised: 5 July 2026
Accepted: 28 July 2026
Published: 30 July 2026

Copyright: © 2026 by the authors. Licensee MDPI, Basel, Switzerland. This article is an open access article distributed under the terms and conditions of the Creative Commons Attribution (CC BY) license.

molecules: ubiquitin-specific protease (*UBP*), ubiquitin C-terminal hydrolase (UCH), OTU-related protease, and Machado–Joseph disease protein domain protease [6,9]. The main deubiquitinases are *UBPs*, which are widely distributed in eukaryotes and are highly conserved in terms of structure and function. These enzymes contain two conserved motifs (cysteine and histidine boxes) [10,11]. Many *UBP*-encoding genes from animals (including humans) and yeast have recently been cloned and expressed [12,13]. Additionally, there has been considerable research on *UBPs* in *Arabidopsis thaliana* [14], which contains 27 *UBP* family genes. In addition to the two conserved regions (cysteine and histidine boxes), there are some special structures in *UBP* proteins, including the MYND finger structure, UBA structure, and MATH domain [14,15]. *AtUBP* genes have been further divided into 14 subfamilies according to the structural differences in the encoded proteins. Because of their special structures, these enzymes are involved in diverse signaling pathways during plant development [16–18].

The *UBP* gene family was reported to be involved in plant growth and development. In *Arabidopsis thaliana*, the *AtUBP15* gene regulates seed and organ size by interacting with ubiquitin receptor DA1, controls plant branching by interacting with CUC2/CUC3-DA1, and regulates petal size and fertility by interacting with ask [19–21]. *AtUBP14* interacts with ultraviolet-B-insensitive 4 to regulate endoreduplication and cell and organ growth, and regulates endoreduplication and cell organ growth through the CDKB1;1-CDKG2/SUD6 cascade [22,23]. Moreover, *AtUBP14* is involved in early embryo development and responses to phosphate deficiency [24,25]. Previous studies have also shown that *UBP* genes are involved in some hormone signaling and stress. For example, *AtUBP24* plays a negative regulatory role in abscisic acid signaling [26]. *AtUBP12* and *AtUBP13* positively regulate brassinosteroid response [27]. *ZmUBP15*, *ZmUBP16*, and *ZmUBP19* have been reported to have an important role in tolerance to cadmium stress and salt stress [28]. *OsUBP21* negatively regulates heat stress [29].

P. mume is an important ornamental tree species used for landscaping worldwide. In China, it has been used for more than 7000 years and has been cultivated for more than 3000 years [30]. The published *P. mume* genome sequence provides important data for identifying genes associated with fine ornamental traits and stress resistance [31]. Low temperatures are particularly important for *P. mume*. Among them, low temperatures are the decisive factor for bud dormancy and its augmentation in *P. mume* [32]. The flowering rate, flower diameter, flowering quantity, flowering uniformity, and bud development are impacted by low-temperature accumulation [33]. After experiencing low temperatures, the petals of *P. mume* 'Meiren' fade and wilt, resulting in low ornamental value [34]. Different varieties of *P. mume* were treated under low-temperature stress for different periods of time, and it was found that the temperature affects the germination rate of the pollen, thereby influencing its productivity [35]. According to the investigations of *P. mume* cultivars in six provinces, several new cold-resistant cultivars were selected and introduced, for example, 'Yanwen Fenghou', 'Yulong Hongfei', 'Judian No. 1', and so on [36]. Previous studies have analyzed *UBP* genes in many plants [14,37], but *P. mume UBP* genes have not been thoroughly investigated. Thus, in this study, 30 *PmUBP* genes were identified and characterized in terms of their conserved domains, phylogenetic relationships, genomic structures, motif distribution, syntenic relationships, tissue-specific expression patterns, promoter cis-acting elements, and responses to low-temperature stress. The study results provide the basis for future research on *P. mume UBP* gene functions in regard to low-temperature stress.

2. Materials and Methods

2.1. Identification and Analysis of Conserved Domains Encoded by PmUBP Genes

P. mume genome data were obtained from the BioProject database (accession number PRJNA171605) [30]. The HMM profile of the UCH domain (accession number PF00443) was downloaded from the Pfam database (http://pfam.xfam.org/, accessed on 23 July 2024). This profile was used as a query to search against the *P. mume* genome dataset using HMMER, with the threshold set to 1×10^{-5}. The retrieved candidate sequences were subsequently subjected to further analysis using the online NCBI-CDD program (https://www.ncbi.nlm.nih.gov/, accessed on 24 July 2024). Sequences lacking the conserved UCH domain were excluded. For multiple isoforms from the same locus, only the longest isoform with complete UCH domain was selected as canonical sequence for subsequent analysis.

PmUBP genes were named according to their relative chromosomal positions. Moreover, specific features of the encoded proteins, including protein length, MW, and theoretical pI, were analyzed using Expasy tools (https://web.expasy.org/protparam/, accessed on 29 July 2024) [38].

2.2. Construction of a Phylogenetic Tree

A phylogenetic tree was constructed for the *P. mume* and *Arabidopsis thaliana UBP* gene families using MEGA software version 6.0 [39]. *PmUBP* and *AtUBP* protein sequences were obtained from the National Center for Biotechnology Information (NCBI) and TAIR databases, respectively. Information for *AtUBPs* is listed in Table S1. The sequences were aligned using MUSCLE, and a phylogenetic tree was constructed using the maximum-likelihood method with 500 bootstrap replicates and Jones–Taylor–Thornton (JTT) model [40].

2.3. Analyses of Genomic Structure and Motif Distribution

PmUBP and *AtUBP* coding regions and genomic sequences were downloaded from the BioProject database. Genomic structures were analyzed using GSDS 2.0 (http://gsds.gao-lab.org/, accessed on 8 October 2024) [41]. Multiple Expectation Maximization for Motif Elicitation (MEME) Suite v5.5.4 was used to identify conserved protein motifs across all target UBP sequences [42]. The key parameter settings were fully specified as follows: the minimum and maximum motif widths were set to 6 and 50 amino acids, respectively; zoops (zero or one occurrence per sequence) was chosen as the site distribution model; the maximum number of distinct motifs to discover was limited to 10; and the statistical significance threshold for retaining candidate motifs was set to an E-value $< 1 \times 10^{-5}$.

2.4. Chromosomal Localization and Synteny Analysis

A chromosomal map was drawn according to the *PmUBP* genome data using MapDraw [43]. Protein and CDS sequences from the genome versions *P. mume* v1.0 under BioProject PRJNA171605, *Prunus persica* v2.0, *Prunus avium* v1.0, and *Prunus armeniaca* were downloaded to conduct cross-species orthology analysis, where only primary assembly scaffolds and chromosomes were kept while unplaced small contigs were discarded. All-versus-all BLASTP 2.13.0+ was run for preliminary screening with an E-value threshold of 1×10^{-5}, a minimum alignment length of no less than 50 amino acids, and query coverage above 30% to eliminate low-confidence homologous gene pairs. Collinear blocks were identified by MCScanX with adjusted core default parameters including a match score no lower than 5, a gap penalty of -1, and a maximum of 10 permissible gaps between adjacent gene pairs, and only blocks harboring at least three collinear gene pairs were reserved for subsequent analyses [44]. Intraspecies duplication types within the *P. mume* genome were divided into two categories, with tandem duplication referring to

two duplicated genes situated within a 200 kb chromosomal interval without any intervening non-homologous genes and segmental duplication referring to homologous gene pairs mapped to independent collinear blocks on different chromosomes or scaffolds with a physical distance exceeding 200 kb, while cross-species gene pairs were categorized as orthologs to distinguish them from intraspecies tandem and segmental duplicates. All collinearity results were displayed via the Dual Systeny Plotter [45]. The coding sequences of intraspecies duplicated gene pairs and interspecies orthologous gene pairs were subjected to codon-level alignment using MUSCLE; the nonsynonymous substitution rate Ka, synonymous substitution rate Ks, and Ka/Ks ratios were computed with the MA model implemented in KaKs_Calculator 2.0 [46]. Standardized data filtering was applied prior to selection pressure and divergence time evaluation; gene pairs with a Ks value of zero or uncomputable Ka/Ks ratios were removed since incomplete data cannot sustain reliable evolutionary deduction, and gene pairs with Ks values greater than 2.0 were considered to have undergone synonymous site saturation such that their corresponding divergence times were only recorded as coarse estimates instead of exact dating results. Divergence time was calculated based on the formula $T = Ks/2\lambda$, where λ equals 1.26×10^{-8} substitutions per site per year, and all divergence time values derived from high-Ks gene pairs were clearly labeled as approximate data in both the main text and Supplementary Tables.

2.5. Analysis of Tissue-Specific Expression Patterns

FPKM values were calculated according to the number of sequenced reads for each transcript. Transcriptome raw data covering five tissues (bud, leaf, root, stem, fruit) were downloaded from NCBI GEO (GSE40162) [30]. Notably, this public dataset contains only one pooled library/sample per tissue without biological replicates, which limits statistical comparison of expression differences across tissues; thus, all tissue expression results herein are used only for a descriptive overview of relative expression trends, rather than for statistical inference of tissue-specific expression. Raw read counts were normalized to FPKM values for each *PmUBP* gene, and all FPKM values are summarized in Supplementary Table S2. Raw FPKM values were subjected to row-wise Z-score normalization (data transformation) to eliminate expression magnitude differences among genes. Hierarchical clustering was performed using Euclidean distance and Ward's linkage method. The 10 expression clusters shown in the heatmap were defined based on the branching structure of the hierarchical clustering tree, grouping genes with highly consistent tissue expression patterns. The heatmap was generated with TBtools 2.007 [47].

2.6. Analysis of Promoter Cis-Acting Elements

The 2000 bp regions upstream of the translation start site of *PmUBP* genome sequences were selected as putative promoter regions. Promoter cis-acting elements were analyzed using PlantCARE (http://bioinformatics.psb.ugent.be/webtools/plantcare/html/, accessed on 6 March 2025) [48].

2.7. Plant Materials and Treatments

One-year-old uniform seedlings of *Prunus mume* cultivar 'Meiren' were used in this study. All seedlings were pre-cultivated in a programmable growth chamber with consistent baseline conditions: constant temperature of 25 °C day/20 °C night, 12 h light/12 h dark photoperiod, photosynthetic photon flux density of 150 $\mu mol \cdot m^{-2} \cdot s^{-1}$, air relative humidity 65%–70%, and soil volumetric moisture maintained at 60%–70%. Seedlings were acclimated to these baseline growth conditions for 14 days before cold treatment to eliminate environmental fluctuation interference. Seedlings remained at the initial baseline temperature (25 °C day/20 °C night) without cold exposure; stem tissues were harvested at identical time points (6, 12, 24, 48 h) corresponding to cold treatments to

exclude circadian rhythm and cultivation duration effects. For the chilling stress group, the chamber temperature was reduced at a constant cooling rate of 2 °C/h until reaching 4 °C, then held at constant 4 °C for 48 h of continuous treatment. In this study, 4 °C was selected as the chilling stress temperature because it is the typical low non-freezing temperature that frequently occurs in early spring and late autumn in the main plum-producing areas, which can induce a cold acclimation response and physiological and molecular changes in *P. mume* without causing ice crystal formation in plant cells; it is also the optimal temperature for studying the cold tolerance adaptation mechanism of woody ornamental plants under mild low-temperature stress. For the freezing stress group, after the same 2 °C/h cooling ramp to 4 °C (4 h cold acclimation), the temperature was further decreased at 2 °C/h to −20 °C and maintained for up to 48 h. The temperature of −20 °C was chosen as the severe freezing stress condition, which simulates the extremely low-temperature freezing environment in winter in northern plum-growing regions. It should be noted that −20 °C represents extreme low-temperature treatment; prolonged exposure may cause cell membrane rupture and tissue necrosis. Since we did not detect physiological indicators such as relative electrolyte leakage (membrane integrity) or leaf cell viability in this study, the observed transcriptional fluctuations only reflect molecular responses triggered by severe freezing injury, rather than adaptive cold acclimation signals. For each sampling time point (6, 12, 24, 4, and 8 h after the target temperature was reached), healthy current-year stem segments (1–2 cm) were collected. Stems were selected as the research material in this study for the following reasons. As the main structural and transport organ of woody *P. mume* seedlings, stems are directly exposed to low-temperature stress in the natural growth environment, with weak cold resistance and a sensitive response to low temperature. Moreover, stems bear the key functions of water and nutrient transportation and mechanical support for plants, and their physiological and molecular changes under cold stress can directly reflect the overall cold tolerance level of *P. mume* seedlings, which is more representative than leaves and roots for evaluating the cold resistance of woody perennial plants. Each biological replicate contained stem tissues pooled from 6 independent uniform seedlings; three fully separated biological replicates were set for every group and time point to ensure statistical reliability. All sampled tissues were immediately snap-frozen in liquid nitrogen and stored at −80 °C prior to total RNA extraction.

2.8. Transcriptome Sequencing and Bioinformatics Analysis

After completion of the above treatments, total RNA extraction, library construction, and Illumina PE150 sequencing were performed, and all raw sequencing FASTQ data were submitted to NCBI SRA database (Accession: PRJNA1483443). Sample names, treatment groups and replicate information were summarized in Supplementary Table S3.

Raw sequencing reads were quality-controlled with FastQC v0.11.9, and low-quality data were filtered via Trimmomatic v0.39: adapters were removed, and reads with average Phred score < 20 and length < 50 bp were discarded. Clean reads were mapped to the official *Prunus mume* v1.0 reference genome using HISAT2 v2.2.1; mapping statistics including total clean reads and uniquely mapped read ratios for each sample were listed in Supplementary Table S4. Gene-level raw integer read counts were quantified with featureCounts v2.0.6.

Differential expression analysis was performed using DESeq2 v1.46.0. Only raw unnormalized read counts were used as DESeq input. Genes with average raw count < 1 across all samples were pre-filtered to reduce noise. Multiple testing correction was conducted via the Benjamini–Hochberg method to control false discovery rate (FDR). Genes with

adjusted p-value (Padj) < 0.05 and |log2(fold change)| ≥ 1 were identified as differentially expressed genes (DEGs).

2.9. RNA Extraction and Quantitative Real-Time Polymerase Chain Reaction (qRT-PCR) Analysis

Total RNA was extracted from hormone-treated samples using the RNAprep Pure Plant Plus Kit (Tiangen, Beijing, China). The extracted RNA was reverse transcribed to generate cDNA using EasyScript® One-Step gDNA Removal and cDNA Synthesis SuperMix (TransGen Biotech, Beijing, China). Based on the heat map, 13 genes with high expression were selected for qRT-PCR analysis. *PmUBP*-specific qRT-PCR primers (Table S5) were designed using Primer Premier 5 software. Additionally, cDNA obtained via reverse transcription was used as the qRT-PCR template. Specifically, qRT-PCR was completed using a reaction volume comprising 2 µL template, 10 µL 2× TransStart® Tip Green qPCR SuperMix (TransGen Biotech), 7.2 µL ddH_2O, and 0.4 µL forward and 0.4 µL reverse primers (200 nM). The *P. mume* phosphatase 2A-encoding gene (PP2A) was selected as a reference gene [49–51]. qRT-PCR was performed on Bio-Rad CFX96 (Hercules, CA, USA) using a two-step cycling protocol: initial denaturation at 95 °C for 2–3 min, followed by 40 cycles of 95 °C for 15 s and 60 °C for 30 s with fluorescence signal collection. The amplicon sizes ranged from 150 to 250 bp. No-template control (NTC) as the unified negative control for all RT-qPCR amplifications. Three biological replicates were set for each treatment, and statistical analysis was conducted based on ΔCt. For statistical analysis, one-way ANOVA was conducted, followed by Duncan's multiple range test.

3. Results

3.1. Identification and Analysis of UBP Genes in P. mume

Thirty *PmUBP* genes were identified based on the *P. mume* genome (Table 1). These genes were named according to their relative chromosomal positions. Moreover, Expasy tools were used to analyze the encoded proteins and determine their physicochemical properties, including molecular weight (MW) and isoelectric point (pI). *PmUBP* coding regions ranged from 315 bp (PmUBP5) to 4833 bp (PmUBP23). An analysis of the encoded proteins indicated that most PmUBPs (73%) comprised 500–1120 amino acids (aa), with a pI of 4.60–9.74. Among the *PmUBP*s, *PmUBP5* and *PmUBP23* had the lowest (11,539.67 Dalton) and highest (181,119.35 Dalton) MW, respectively.

Table 1. Details regarding *PmUBP* genes.

Gene Name	Gene ID	Chromosomal Location	CDS Length (bp)	Protein		
				Length	pI	MW (Da)
PmUBP1	103329759	LG1: 11,162,374–11,176,244	2634	877	5.64	98,944.93
PmUBP2	103329910	LG1: 11,462,041–11,479,163	3345	1114	5.59	130,579.66
PmUBP3	103333030	LG1: 15,748,055–15,752,876	1107	368	5.88	42,000.37
PmUBP4	103334293	LG1: 17,053,005–17,058,538	2481	826	8.67	91,990.39
PmUBP5	107880421	LG2: 1,279,108–1,280,159	315	104	9.50	11,539.67
PmUBP6	103319511	LG2: 4,977,117–4,984,850	3330	1109	8.18	120,900.17
PmUBP7	107880447	LG2: 5,337,266–5,338,732	459	152	9.74	16,928.18
PmUBP8	103319991	LG2: 8,123,859–8,131,835	3264	1087	5.62	122,288.52
PmUBP9	103320674	LG2: 11,964,899–11,970,108	2103	700	6.06	77,224.76
PmUBP10	103320713	LG2: 12,282,409–12,285,771	1662	553	8.44	63,019.80
PmUBP11	103324251	LG2: 41,336,214–41,342,214	2904	967	5.35	105,976.73
PmUBP12	103325824	LG3: 9,336,111–9,343,655	3012	1003	7.93	112,541.52
PmUBP13	103325842	LG3: 9,517,281–9,524,424	2184	727	9.35	79,859.25
PmUBP14	103326292	LG3: 12,632,216–12,640,640	2430	809	5.00	89,619.32
PmUBP15	103326991	LG3: 20,786,851–20,792,307	1704	567	5.60	65,988.45
PmUBP16	103327733	LG4: 3,672,419–3,678,152	1431	476	5.93	53,615.82

Table 1. *Cont.*

Gene Name	Gene ID	Chromosomal Location	CDS Length (bp)	Protein		
				Length	pI	MW (Da)
PmUBP17	103330738	LG5: 2,896,759–2,902,722	1626	541	7.15	58,654.40
PmUBP18	103331020	LG5: 6,510,250–6,527,422	3360	1119	5.49	131,386.42
PmUBP19	103336756	LG7: 1,172,882–1,178,278	1686	561	6.19	65,094.79
PmUBP20	103336892	LG7: 3,394,042–3,398,169	2169	722	5.52	79,315.57
PmUBP21	107881550	LG7: 5,340,557–5,344,660	582	193	4.60	21,226.36
PmUBP22	103337879	LG7: 11,487,068–11,495,122	2790	929	5.46	105,153.78
PmUBP23	103338359	LG7: 13,387,324–13,395,850	4833	1610	5.53	181,119.35
PmUBP24	103339556	LG8: 7,429,063–7,438,849	2823	940	5.08	106,975.67
PmUBP25	103339587	LG8: 7,790,584–7,801,578	3354	1117	5.64	131,128.46
PmUBP26	103341262	LG8: 16,741,043–16,748,940	2865	954	9.45	104,728.60
PmUBP27	103342897	scaffold82: 76,893–89,850	2817	943	5.88	106,189.56
PmUBP28	107881879	scaffold82: 90,288–91,061	456	151	8.73	17,526.00
PmUBP29	103342763	Scaffold188: 62,878–69,329	1719	572	6.01	64,139.92
PmUBP30	103344261	Scaffold: 55–1927	963	320	6.19	36,341.02

3.2. Analyses of Conserved Domains and Phylogenetic Relationships of PmUBP Genes

Conserved domains in *PmUBP*s and *AtUBP*s were analyzed according to their protein sequences. The results indicated that members of the same subfamily had similar conserved domains (Figure 1). All *PmUBP*s contained the UCH domain, which is a typical conserved domain in the UBP family [6]. The *PmUBP*s with only one conserved domain (i.e., UCH) included *PmUBP13*, *PmUBP26*, *PmUBP20*, *PmUBP8*, *PmUBP3*, *PmUBP17*, *PmUBP21*, *PmUBP29*, *PmUBP7*, *PmUBP5*, *PmUBP28*, *PmUBP24*, and *PmUBP1*. The *PmUBP*s with two conserved domains included *PmUBP4*, *PmUBP6*, *PmUBP9*, *PmUBP12* (UCH and zf-MYND), *PmUBP10*, *PmUBP11*, *PmUBP15*, *PmUBP19* (UCH and zf-UBP), *PmUBP16* (UCH and ubiquitin), *PmUBP22*, and *PmUBP27* (UCH and DUSP). Three conserved domains were detected in *PmUBP14* (UCH, zf-UBP_var, and zf-UBP) and *PmUBP23* (UCH, DUF627, and DUF629). *PmUBP2*, *PmUBP18*, and *PmUBP25* had four conserved domains (UCH, MATH, USP7_1CP0_bdg, and USP7_C2).

To clarify the evolutionary relationships among *PmUBP*s, a phylogenetic tree was constructed on the basis of the full-length amino acid sequences of 30 *PmUBP*s and 27 *AtUBP*s (Figure 2). According to the verified *AtUBP*s, 30 *PmUBP*s were divided into 16 groups, most of which consisted of only one *PmUBP*. Some groups contained two or three *PmUBP*s (e.g., G1, G8, and G11). Notably, G16 was the largest group (seven *PmUBP*s).

3.3. Chromosomal Localization and Synteny Analysis of PmUBP Genes

According to chromosomal location information, 26 *PmUBP* genes were mapped to seven chromosomes, whereas four *PmUBP* genes were mapped to three scaffolds (Figure 3A). Thus, the *PmUBP* genes were broadly distributed among chromosomes. Chromosome LG2 had seven *PmUBP* genes, which was more than any other chromosome. There were four *PmUBP* genes on chromosomes LG1 and LG3, five *PmUBP* genes on chromosome LG7, two *PmUBP* genes on chromosome LG5 and scaffold82, and three *PmUBP* genes on chromosome LG8. Chromosome LG4 and scaffold188 had only one *PmUBP* gene each.

Genome replication, tandem replication, segmental replication, and transposon replication are all replication events contributing to plant evolution [52]. Hence, *PmUBP* gene replication events were analyzed on the basis of aligned sequences and relative chromosomal positions. Duplication events played an important role during the expansion of the *PmUBP* family. Among the 30 *PmUBP* genes, the following three gene pairs were derived from segmental duplications: PmUBP1 and PmUBP24, PmUBP2 and PmUBP25, and PmUBP4 and PmUBP7 (Figure 3A). Holub reported that two duplicated genes within

a 200 kb chromosomal region were the result of a tandem duplication [53]. Accordingly, one *PmUBP* gene pair (PmUBP27 and PmUBP28) on scaffold82 was likely the result of a tandem duplication. To elucidate the selection pressure on the *PmUBP* family, Ka (nonsynonymous substitution), Ks (synonymous substitution), and Ka/Ks values were calculated (Table S6). Generally, Ka/Ks values greater than, equal to, and less than 1 represent positive, neutral, and negative selection, respectively [54,55]. After filtering gene pairs with undefined Ka/Ks values, all intraspecies segmental duplication pairs (*PmUBP1–PmUBP24*, *PmUBP2–PmUBP25*, *PmUBP4–PmUBP7*) exhibited Ka/Ks < 1, consistent with purifying (negative) selection. According to the calculated T values (Table S1), the divergence times of the *PmUBP1–PmUBP24* and *PmUBP27–PmUBP28* gene pairs were 124.07 and 2.02 million years ago (Mya), respectively.

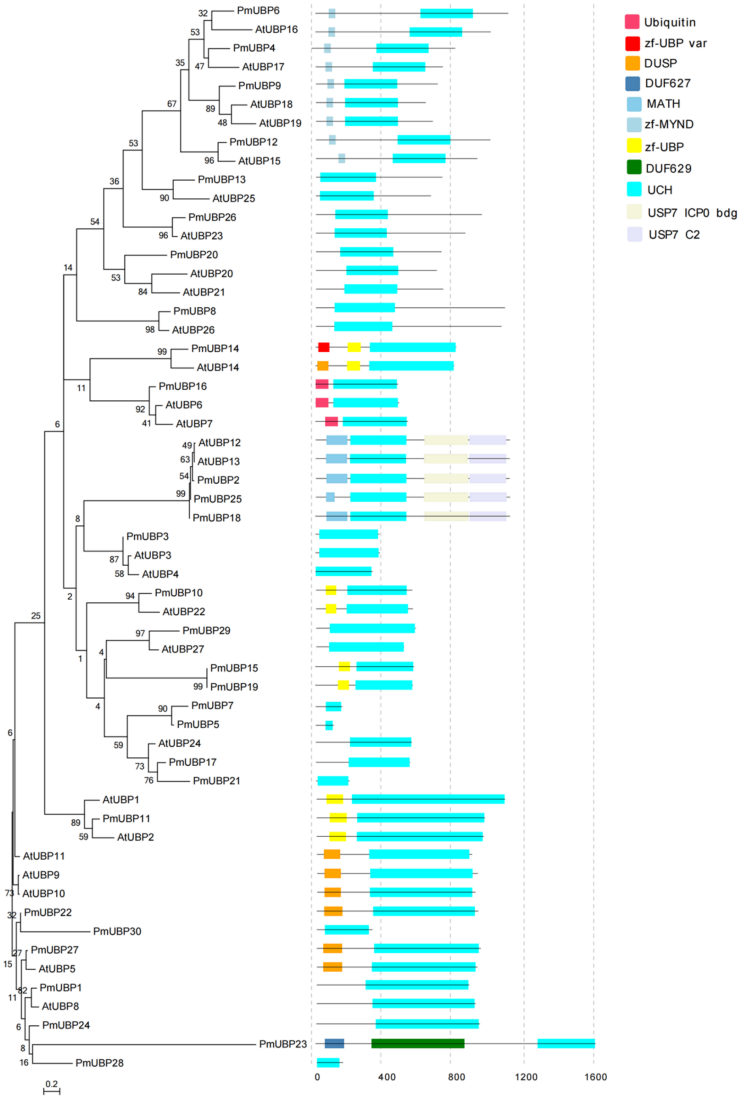


Figure 1. *PmUBPs* and *AtUBPs* conserved domains. Different conserved domains are represented by different colored boxes. Box length represents domain length. The numbers represent branch lengths.

To further explore the evolution of the *PmUBP* gene family, we constructed synteny maps to clarify how *P. mume* is associated with *P. persica*, *P. avium*, and *P. armeniaca* (Figure 3B–D). A total of 29, 28, and 27 syntenic orthologous gene pairs were identified between *P. mume* and *P. persica*, between *P. mume* and *P. avium*, and between *P. mume* and *P. armeniaca*, respectively. Collinearity was detected between some *PmUBP* genes and two *PpUBP* or *PaUBP* genes. For example, *PmUBP14*, *PmUBP16*, *PmUBP21*, and *PmUBP22*

were associated with *PpUBP* genes, and *PmUBP12*, *PmUBP14*, and *PmUBP16* were associated with *PaUBP* genes. The Ka, Ks, Ka/Ks, and T values of these syntenic orthologous gene pairs in the three species were calculated (Table S6). All gene pairs had a Ka/Ks value less than 1, ranging from 0.02 to 0.72, indicating that *PmUBP* genes evolved under negative selection pressure along with *PpUBP*, *PaUBP*, and *PamUBP* genes. The divergence times between *P. mume* and *P. persica* gene pairs ranged from 0.60 to 60.16 Mya, with most of the duplicated gene pairs appearing 0.6–2.5 Mya (76%). In contrast, the divergence times between *P. mume* and *P. avium* gene pairs ranged from 1.04 to 60.16 Mya, with most gene duplication events occurring 1–4.5 Mya (79%). Additionally, chromosomes 1, 2, 3, 5, 7, and 8 had the most syntenic gene blocks. In contrast, there were relatively few syntenic *UBP* gene blocks on chromosomes 4 and 6.

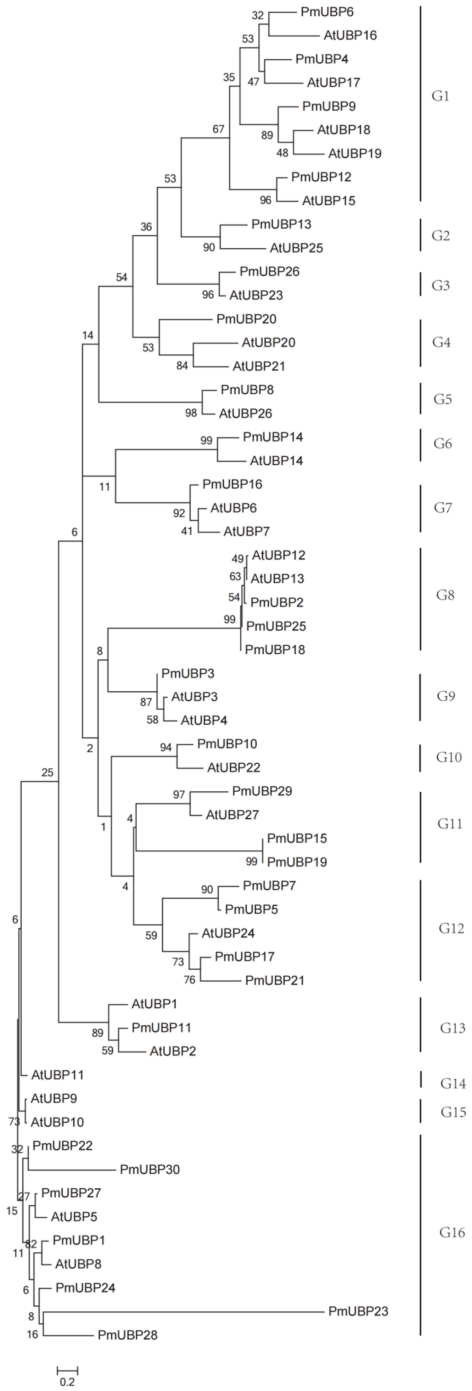


Figure 2. Phylogenetic tree of *PmUBP*s and *AtUBP*s. The numbers represent branch lengths.

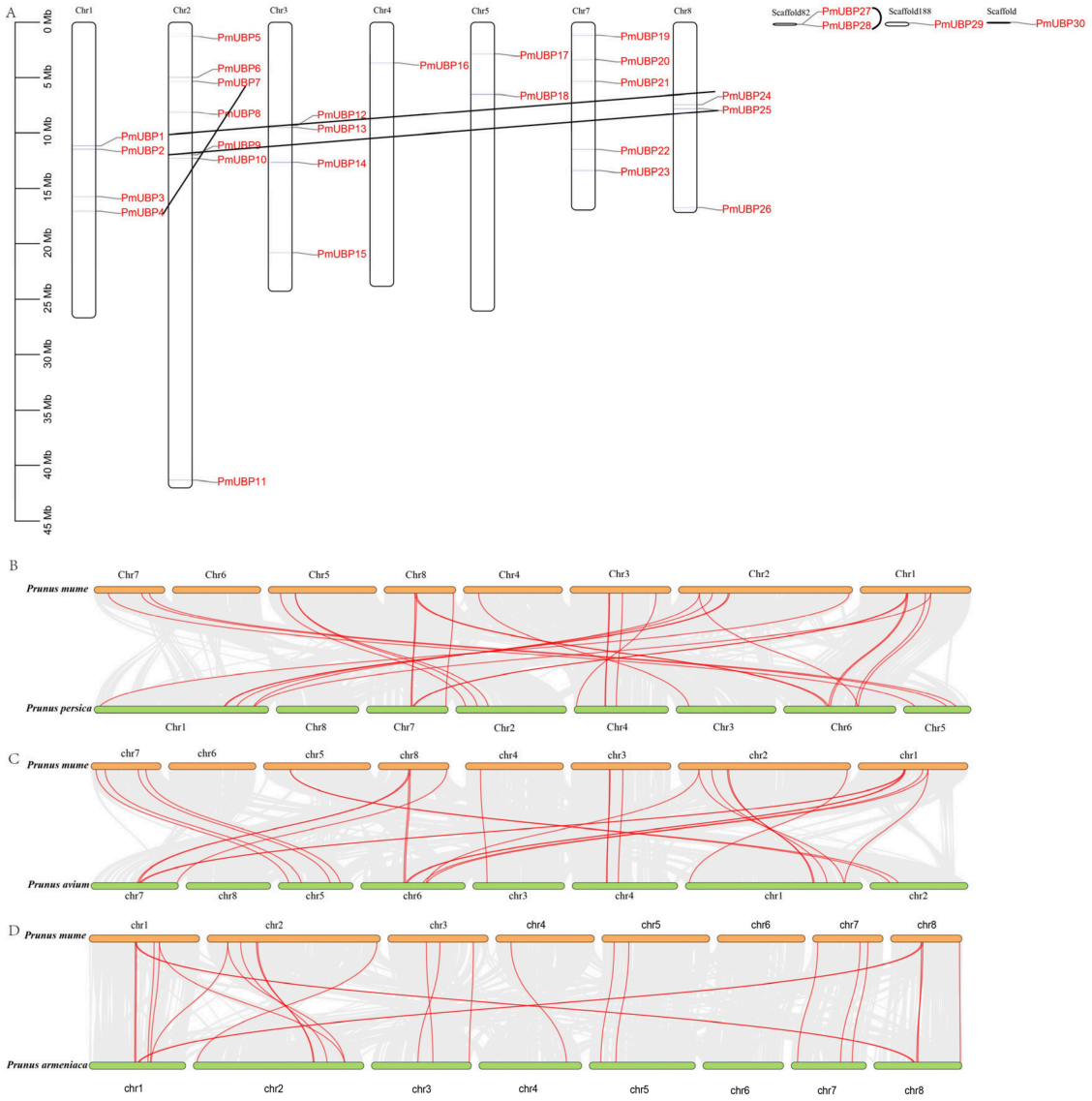


Figure 3. Chromosomal map of *PmUBP* genes and synteny between *Prunus* species. (**A**) Chromosomal map revealing the locations of 30 *PmUBP* genes. Segmentally and tandemly duplicated gene pairs are indicated with connecting lines. (**B**) Synteny analysis of *P. mume* and *P. persica*. (**C**) Synteny analysis of *P. mume* and *P. avium*. (**D**) Synteny analysis of *P. mume* and *P. armeniaca*.

3.4. Genomic Structure and Conserved Motif Analyses of PmUBP Genes

To investigate the evolutionary relationships between *P. mume* and *Arabidopsis thaliana UBP* gene families, *PmUBP* and *AtUBP* gene structures were analyzed (Figure 4). The *PmUBP* and *AtUBP* genes had 2–32 exons and 1–31 introns. Most of the analyzed genes contained an untranslated region (UTR). However, some genes lacked a 5′-UTR (*AtUBP1*, *PmUBP30*, and *AtUBP8*), and some genes lacked a 3′-UTR (*PmUBP6*, *PmUBP18*, and *PmUBP2*). Notably, *PmUBP21* lacked both a 5′-UTR and a 3′-UTR. Furthermore, members of the same subgroup had similar genomic structures. For example, G12 genes had a 5′-UTR, 16 exons, 15 introns, and a 3′-UTR.

Using MEME Suite, we detected 10 motifs of varying lengths (11–50 aa) in *P. mume* and *Arabidopsis thaliana UBP*s (Figure 4). Specific details regarding these 10 motifs are provided in Figure S1 and Table S7 (e.g., sequence information, E-value, and logo images). Most *PmUBP*s contained at least five conserved motifs; the exceptions were *PmUBP21*, *PmUBP7*, *PmUBP5*, *PmUBP28*, and *PmUBP23*. Motif 1 was detected in all *PmUBP*s, except for *PmUBP28*. Interestingly, motif 2 was detected twice in *PmUBP28*. These findings,

combined with the results of an analysis of conserved motifs in *Arabidopsis thaliana UBP*s, indicated that the conserved motifs of closely related proteins were similar, but there were substantial differences in the conserved motifs among subgroups.

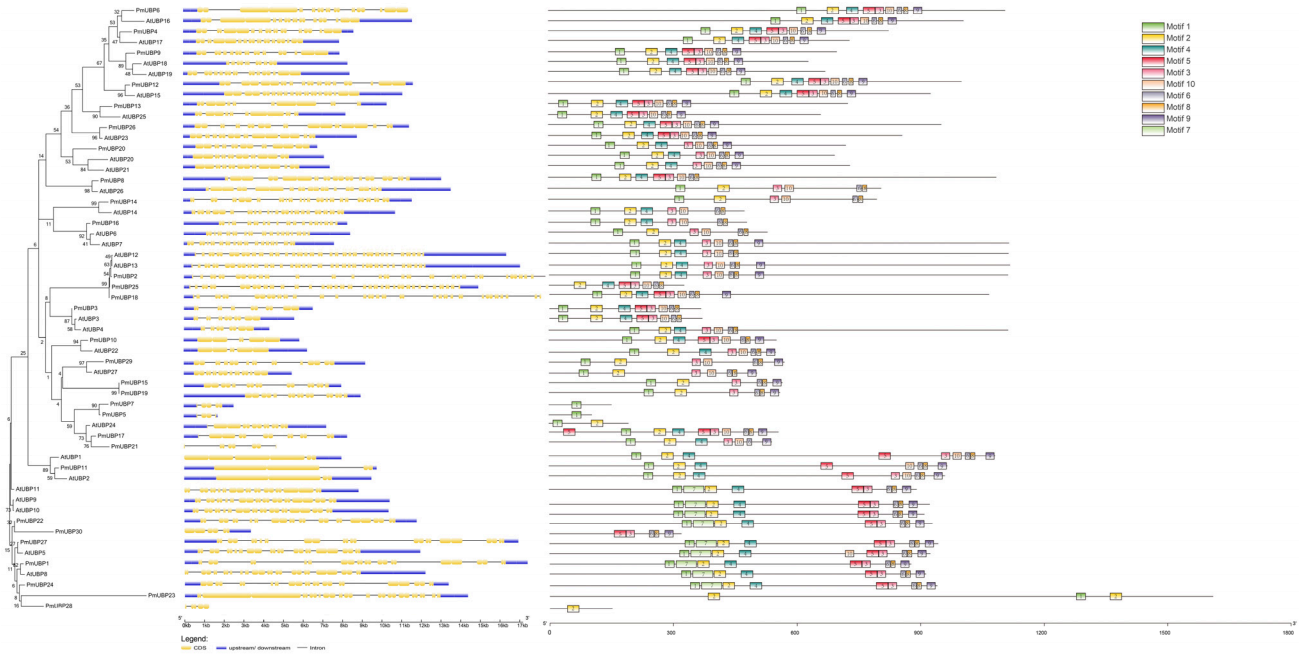


Figure 4. Evolutionary relationships, genomic structures, and motif distribution of *PmUBP* and *AtUBP* genes. *The numbers represent branch lengths.*

3.5. PmUBP Expression Patterns in Different Tissues

Published transcriptome data for five tissues (bud, leaf, root, stem, and fruit) [23] were used to analyze *PmUBP* expression patterns (Figure 5). All raw FPKM values for each gene–tissue combination are provided in Supplementary Table S2, which clearly annotates the tissue source of each sample and establishes a one-to-one correspondence between gene LOC identifiers and *PmUBP* nomenclature. Among the 30 *PmUBP* genes, only *PmUBP21* and *PmUBP5* had undetectable expression levels in the five examined tissues. Additionally, *PmUBP28* expression was undetectable in the bud, leaf, and root, whereas *PmUBP7* was not expressed in the stem. The other 26 *PmUBP* genes were expressed in all tissues (fragments per kilobase of exon per million fragments mapped (FPKM) value > 0). *PmUBP26* exhibited the maximum FPKM value in leaf tissue (197.99), followed by fruit (174.33), stem (101.10), root (94.61), and bud (40.17). However, expression patterns differed among the analyzed genes. According to a cluster analysis, the 30 *PmUBP* genes were divided into 10 groups according to their expression patterns. Group 1 genes were most highly expressed in the leaf and stem. Group 4 genes had the lowest expression levels in the five tissues.

3.6. Analyses of Cis-Acting Regulatory Elements

To explore potential regulatory mechanisms, cis-acting elements within the translation start site 2000 bp upstream promoter regions of the *PmUBP* genes were analyzed using PlantCARE. The analysis revealed a diverse array of regulatory elements distributed across these promoters, including hormone-responsive elements associated with abscisic acid, auxin, gibberellin, MeJA, and salicylic acid, as well as light-responsive and circadian-related elements (Figure 6, Table S8). In addition, various stress-responsive elements were identified, including those involved in anaerobic induction, anoxic responses, defense and stress responses, low-temperature responsiveness, and wound responsiveness. Elements related to tissue-specific expression, particularly in the endosperm and meristem, were also

detected. Notably, hormone-, light-, and stress-responsive elements were highly enriched, suggesting that *PmUBP* genes may play important roles in integrating environmental and hormonal signals.

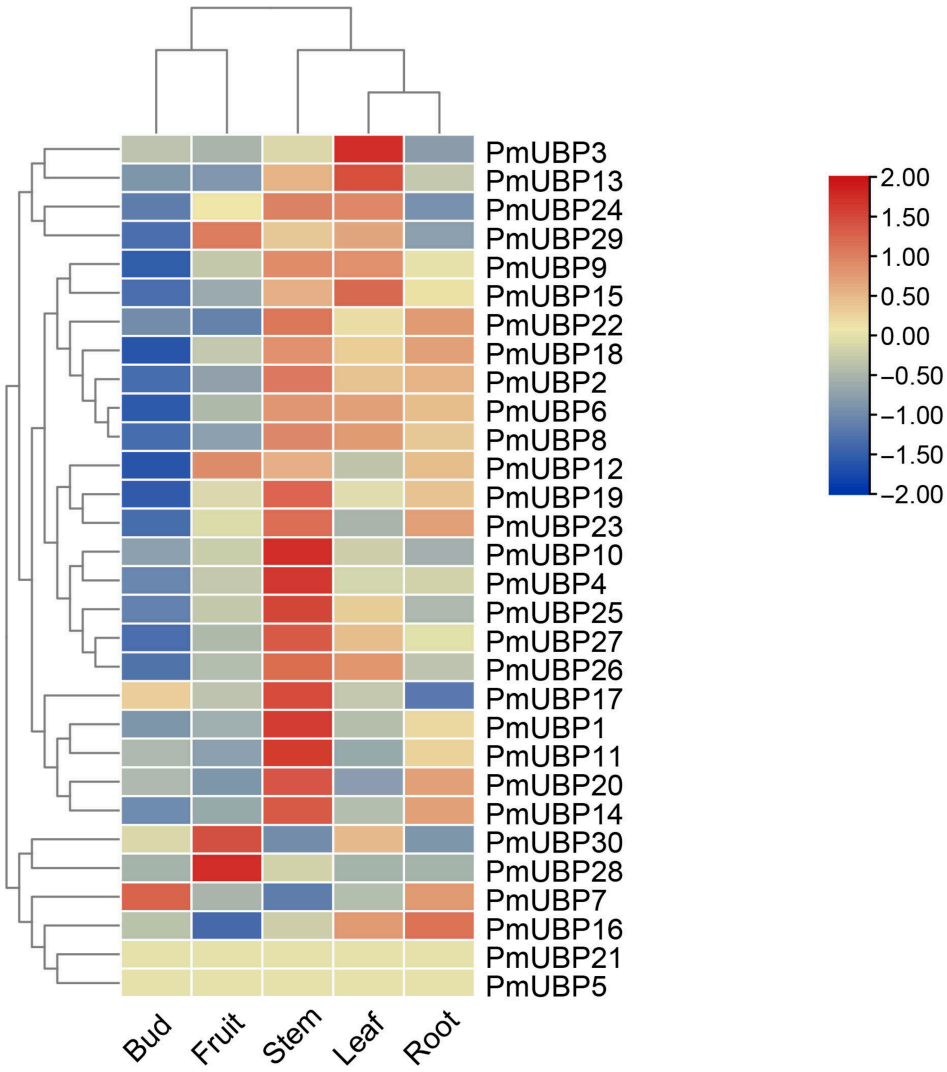


Figure 5. Heat map of expression patterns in different tissues (bud, fruit, stem, leaf, and root). Heat map values are normalized FPKM values ranging from −2 (blue) to 2 (red).

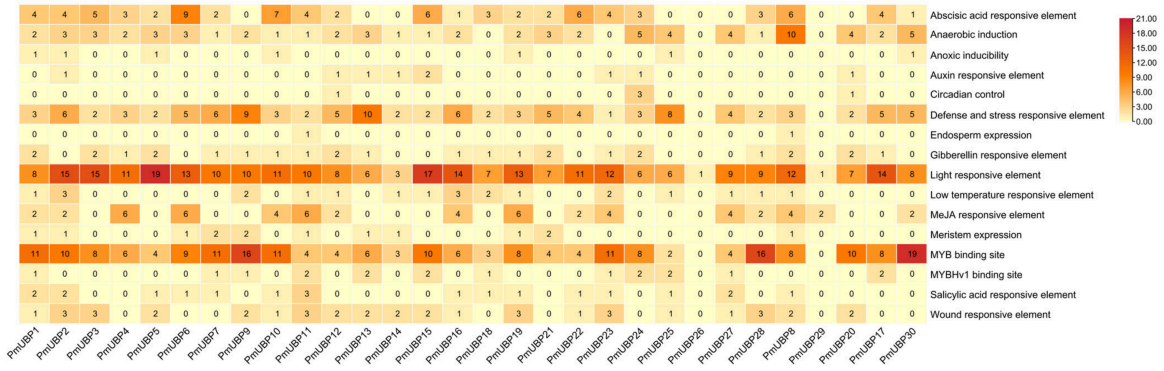


Figure 6. Analysis of cis-acting regulatory elements in the promoters of *PmUBP* genes. Element categories are shown along the rows, including hormone-responsive, light-responsive, stress-responsive, tissue-specific expression-related elements, and transcription factor binding sites, while columns correspond to individual genes (*PmUBP1*–*PmUBP30*). The color scale ranges from yellow to red, representing increasing element abundance, with red indicating higher levels and yellow indicating lower levels.

3.7. Expression Patterns of PmUBP Gene Family Under Low-Temperature Stress Treatment

The *PmUBP* gene family was divided into four subgroups based on expression patterns, comprising a total of 30 genes (Figure 7). Under chilling stress, subgroups I, II, III, and IV included 6, 2, 10, and 12 members, respectively. Genes in ClusterA-I exhibited the highest expression in *Prunus mume*, showing strong overall responses, with all members peaking at 12 h before declining. ClusterA-II displayed the lowest expression levels, exhibiting notable fluctuations, with low expression at 6 h, a transient increase at 12 h, and a subsequent decline at 24 and 48 h. ClusterA-III genes showed generally low and moderate changes, although a few, such as *PmUBP15*, *PmUBP8*, and *PmUBP21*, were slightly upregulated at 12 h. ClusterA-IV genes exhibited relatively high and complex expression patterns, with several members, including *PmUBP20*, *PmUBP2*, *PmUBP22*, and *PmUBP25*, peaking at 12 h.

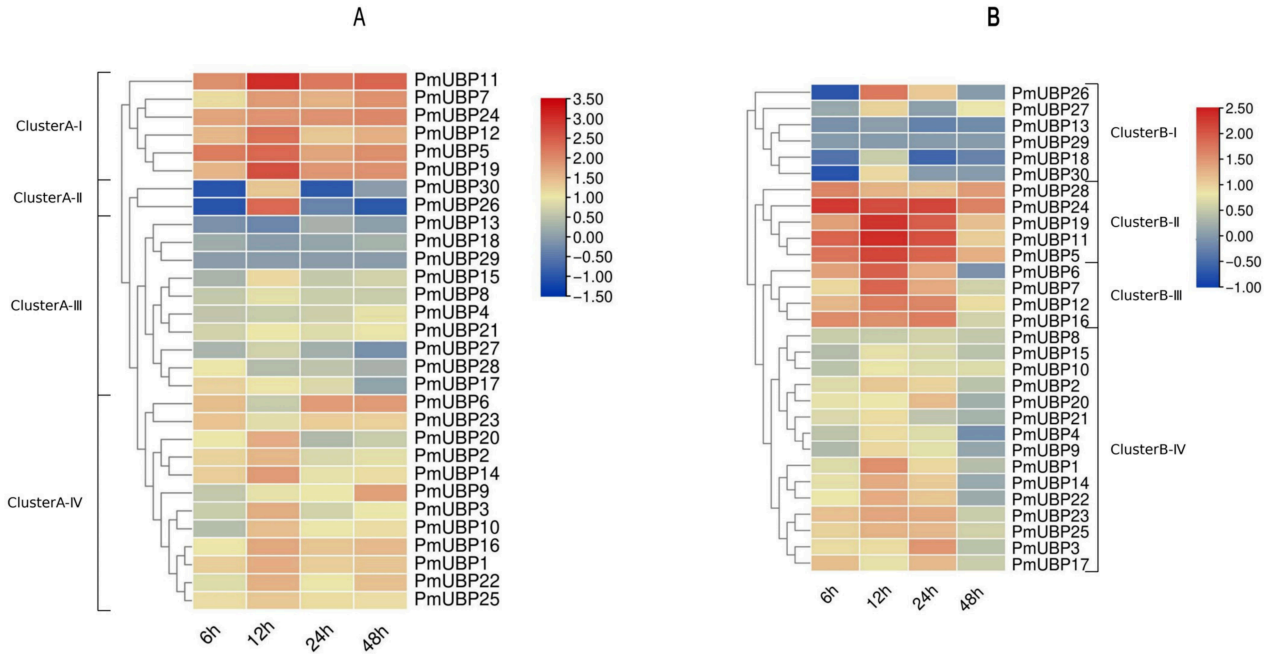


Figure 7. Hierarchical clustering of *PmUBP* gene expression under chilling (4 °C) (**A**) and freezing (−20 °C) (**B**) stress. Time points (6, 12, 24, and 48 h) indicate treatment duration. The heatmap is based on log2 fold change values, with red and blue representing high and low expression levels, respectively.

Under severe freezing stress, subgroups I, II, III, and IV contained 6, 5, 4, and 15 members, respectively. Genes in ClusterB-I maintained low expression across all time points, with pronounced downregulation at 6 and 24 h. In ClusterB-II, most genes, including *PmUBP24*, *PmUBP19*, *PmUBP11*, and *PmUBP5*, were strongly upregulated at 12 h, followed by slight declines. ClusterB-III genes exhibited increased expression at 6, 12, and 24 h, although levels generally decreased by 48 h. ClusterB-IV, the largest group, showed moderate-to-low responses overall, with most genes experiencing mild-to-moderate upregulation at 12 or 24 h and returning to lower levels by 48 h.

3.8. qRT-PCR Analysis of PmUBP Genes Under Chilling and Severe Freezing Stress

To investigate the role of the *PmUBP* gene family in response to chilling and severe freezing stress, the expression patterns of 13 *PmUBP* members were analyzed following exposure to 4 °C and −20 °C at 6, 12, 24, and 48 h (Figure 8). According to the results of chilling stress, *PmUBP2*, *PmUBP11*, *PmUBP13*, *PmUBP18*, and *PmUBP26* were identified as exhibiting the most significant upregulation, for which peak expression was observed

at 48 h (Figure 8A). Among them, the expression level of *PmUBP2* reached approximately 200 times that of the control group within 48 h, making it the most significantly expressed one in this group. Secondly, the expression level of *PmUBP26* reached approximately 100 times that of the control group within 48 h. Finally, the expression levels of *PmUBP11*, *PmUBP13*, and *PmUBP18* reached 15, 20, and 40 times that of the control group, respectively, within 48 h. Under severe freezing stress, *PmUBP2*, *PmUBP11*, *PmUBP13*, *PmUBP18*, *PmUBP22*, and *PmUBP26* genes showed a significantly upward trend compared to the control group (Figure 8B). Among them, *PmUBP26* showed the most significant increase. Its expression level reached approximately 200 times that of the control group within 12 h.

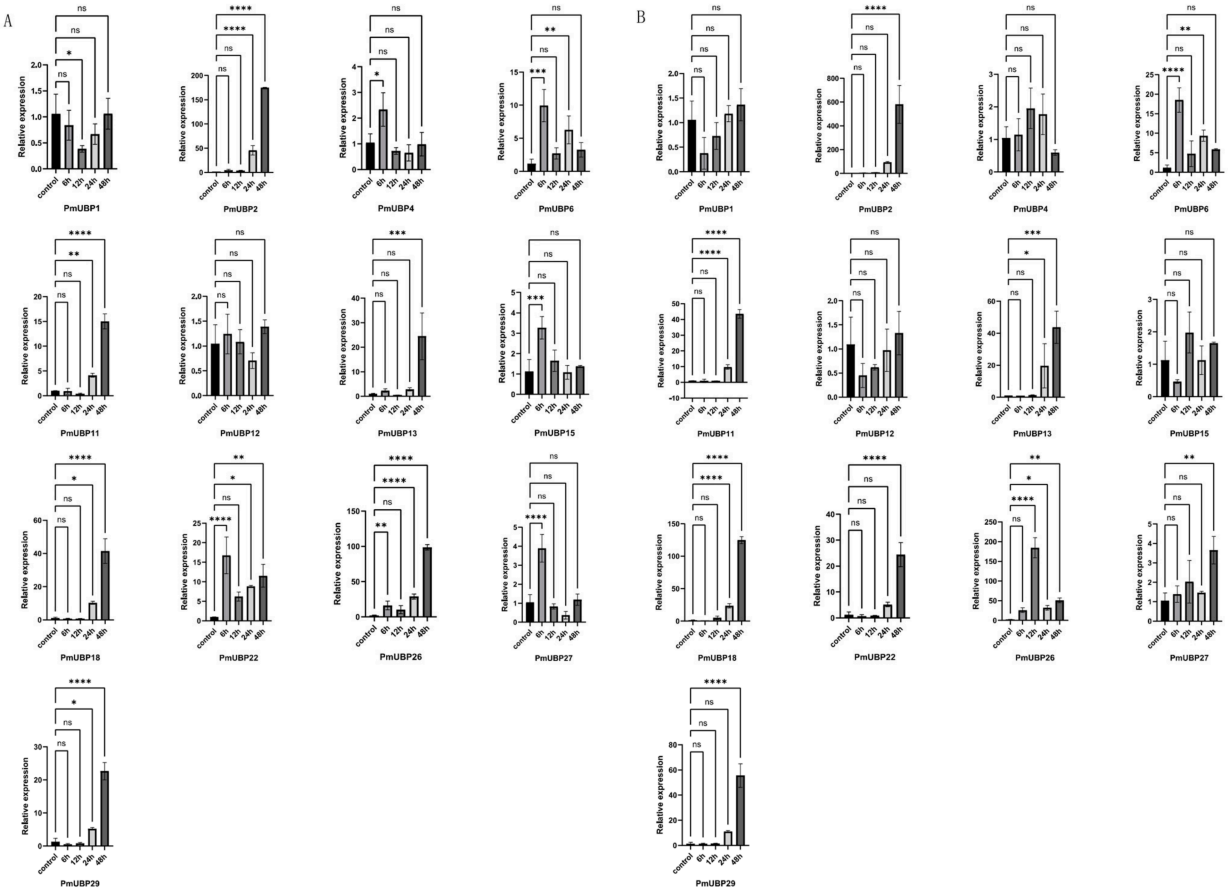


Figure 8. qRT-PCR analysis of *PmUBP* gene expression in *Prunus mume*. The expression patterns of 13 candidate *PmUBP* genes were examined under chilling (4 °C) (**A**) and severe freezing (−20 °C) (**B**) treatments. "Control" represents untreated samples. "6 h", "12 h", "24 h", and "48 h" indicate treatment duration. Error bars represent the standard deviation (SD) of three independent biological replicates. Statistical significance is indicated as follows: ns, $p > 0.05$ (not significant); $p \leq 0.05$ (*); $p \leq 0.01$ (**); $p \leq 0.001$ (***); $p \leq 0.0001$ (****).

4. Discussion

UBP genes are highly conserved in eukaryotes. Previous studies showed that *UBP*s mediate many physiological activities in *Arabidopsis thaliana* [16,18,56,57]. The *UBP* gene family has been identified and characterized in *Arabidopsis thaliana* [14], rice [58], *Brachypodim distachyon*, and other species [59]. However, *P. mume UBP* genes have not been comprehensively identified and characterized. In this study, 30 *PmUBP* genes were identified and classified into 16 subfamilies. The number of *PmUBP* genes did not differ significantly from the number of *UBP* genes in *Arabidopsis thaliana* (27 *AtUBP* genes), rice (25 *OsUBP* genes), *Brachypodium distachyon* (32 *BdUBP* genes), *Moso Bamboo* (48 *PeUBP* genes), and *Quercus robur* (20 *QrUBP* genes), which suggested that *UBP* gene families are conserved among

plant species [11,58–60]. According to an examination of conserved domains, DUF627 and DUF629 are conserved domains in *PmUBP23*, but not in *AtUBPs*. *PmUBP14* contained a unique domain *zf-UBP*_var that does not exist in *AtUBP*s. Interestingly, the *zf-UBP*_var domain also exists in PtrUBP14.1 and *PtrUBP14.2* (*Populus trichocarpa*) [61]. According to the evolutionary relationship analysis, *Arabidopsis thaliana UBP* genes were grouped into 14 subfamilies, whereas *PmUBP* genes were grouped into 16 subfamilies. The core conserved motifs correspond to the classic UCH catalytic domain of UBP proteins and are responsible for deubiquitination activity and protein structural stability, while the variable motif compositions among different subfamilies potentially contribute to functional differentiation and stress-responsive diversity of *PmUBP* genes.

Gene replication events, such as segmental duplications and tandem duplications, can influence the evolution of a species by generating genes with new functions [54,62,63]. In the current study, three *PmUBP* gene pairs were revealed to be the result of segmental duplications, whereas one *PmUBP* gene pair was due to a tandem duplication. Segmental duplications likely contributed to the expansion of the *PmUBP* gene family. To further elucidate *UBP* evolution, syntenic relationships between *P. mume* and *P. persica* and between *P. mume* and *P. avium* were determined. The divergence time was 0.60–60.16 between *P. mume* and *P. persica*, and was 1.04–60.16 between *P. mume* and *P. avium.* A previous study showed that *bHLH* (basic helix–loop–helix) gene duplication events in *P. mume* and *P. persica* began from 0.67 to 86.11 Mya, and in *P. mume* and *P. avium*, they began from 0.14 to 60.81 Mya [64]. The divergence time is similar between *UBP* and *bHLH* gene families, implying that the evolutionary pattern of *UBP* is similar to that of *bHLH* gene families.

The relative tissue expression trends of *PmUBPs* observed from the public transcriptome data provide preliminary clues for exploring the potential roles of these genes in the growth and development of *P. mume*. Analyses of selected tissues (bud, fruit, stem, leaf, and root) indicated that most *PmUBP* genes were highly expressed in the stem and leaf. However, the expression levels of a few genes were similar across the five tissues. For instance, *PmUBP14* was expressed in five tissues, and its homologous gene *AtUBP14* has been reported to be involved in embryo development, endoreduplication, leaf and flower size control, and root hair elongation [22,24,25]. Some *PmUBP* genes had unique tissue expression profiles. For example, *PmUBP30* and *PmUBP28* expression levels were highest in the fruit. Earlier research showed *AtUBP* genes affect cell proliferation and organ size [14,16]. *PmUBP3* was highly expressed in bud tissue. Previous studies have shown that its homologous gene *AtUBP3* is involved in pollen development [56].

Gene promoter cis-acting elements can regulate transcriptional activity by binding to trans-acting factors, thereby modulating plant growth and development [65,66]. In the study, the 2000 bp upstream region of the *PmUBP* coding sequences was analyzed, and multiple cis-regulatory elements were identified, the majority of which were associated with light responsiveness, hormone signaling, and stress responses. These results indicate that *PmUBP* genes may be responsive to a variety of environmental cues. This pattern appears not to be unique to *PmUBP* genes in *P. mume*, as similar regulatory architectures have been reported in other plant species. For instance, the *TaUBP* promoter in *Triticum aestivum* L. has been shown to contain multiple hormone-responsive elements [67], while the *BrUBP* promoter in *Brassica rapa var. oleifera* has been reported to harbor motifs related to low-temperature responsiveness, defense, stress, and light response [68]. In *Capsicum annuum* L., the *CaUBP* promoter similarly contains numerous elements associated with light response, stress response, and hormone signaling [69]. Collectively, these findings suggest that the presence of stress-responsive cis-regulatory elements in *UBP* promoters may be a conserved feature across diverse plant species, which may play a role in the coordinated regulation of *UBP* gene expression under various environmental conditions. In

order to examine the responses of *UBP* genes under low-temperature stress, the expression level of thirteen *PmUBP* genes in *P. mume* was examined. Under cold stress, *PmUBP2*, *PmUBP11*, *PmUBP13*, *PmUBP18*, and *PmUBP26* exhibited relatively pronounced responses, whereas under severe freezing stress, *PmUBP2*, *PmUBP11*, *PmUBP13*, *PmUBP18*, *PmUBP22*, and *PmUBP26* responded more markedly. These results indicate that *PmUBP* genes may be responsive to low-temperature stress, which is consistent with observations in other plant *UBP* gene families. In *Oryza sativa* L., *OsUBP9* and *OsUBP17* have been implicated in both drought and cold tolerance [70].

5. Conclusions

UBP genes are reportedly involved in various growth and developmental processes. In this study, 30 *PmUBP* genes were identified and characterized. An analysis of conserved domains detected UCH in all 30 *PmUBP*s. Notably, proteins in the same subfamily had similar conserved domains. On the basis of the evolutionary relationships of *AtUBP* family members, the 30 *PmUBP* genes were classified into 16 groups. Chromosome maps indicated that these genes were broadly distributed on seven chromosomes and three scaffolds. A synteny analysis identified 29, 28, and 27 syntenic orthologous gene pairs between *P. mume* and *P. persica*, between *P. mume* and *P. avium*, and between *P.mume* and *P. armeniaca*, respectively. Transcriptome-based relative expression profiling showed that 26 out of 30 *PmUBP* genes were detected (FPKM > 0) in all five examined tissues, while *PmUBP5*, *PmUBP7*, *PmUBP21* and *PmUBP28* exhibited tissue-restricted detectable expression. Distinct expression trends across tissues were observed for different *PmUBP* members. *PmUBP* genes respond transcriptionally to the temperature treatments and may therefore be useful candidates for future functional studies.

Supplementary Materials: The following supporting information can be downloaded at: https://www.mdpi.com/article/10.3390/f17080895/s1, Figure S1: The motif logo image of *PmUBPs*. Table S1: The detailed information on *AtUBPs.* Table S2: The FPKM value of PmUBPs from five different tissues. Table S3: Sample names, treatment groups and replicate information. Table S4: Data of mapping statistics. Table S5: The primers of *PmUBPs* for the qRT-PCR experiments. Table S6: The value of Ka, Ks, KaKs, and T. Table S7: The motif detailed information of *PmUBPs*. Table S8: The detailed information on cis-acting elements.

Author Contributions: W.Z. designed the research program, performed the experiment, and wrote the manuscript. W.Z., J.F., J.Z., Y.D., J.M. and X.Z. analyzed the data. The authors all modified the manuscript. All authors have read and agreed to the published version of the manuscript.

Funding: This project is based on research that was supported by the Youth Natural Science Foundation in Shanxi (No. 202203021222415 and 202203021212014), the Key Project of Taiyuan University (23TYZD05), the Talent Recruitment Research Project of Taiyuan University (24TYKY006), and the Joint Funds of the National Natural Science Foundation of China (U2571220).

Institutional Review Board Statement: Not applicable.

Informed Consent Statement: Not applicable.

Data Availability Statement: All data supporting the conclusions of this article are included in the article and its additional files. RNA-sequencing data was uploaded to NCBI database under accession number PRJNA1483443.

Acknowledgments: We greatly appreciate the Forests editors and reviewers for handling our manuscript and providing critical suggestions. We thank MDPI author services (https://susy.mdpi.com/user/author_services/new/revision_email?hash_key=663479f3facb579c5e73c094aac26cb9, accessed on 23 June 2026) for editing the English text of a draft of this manuscript. We appreciate the auxiliary support of artificial intelligence tools in linguistic revision and structural adjustment of the manuscript.

Conflicts of Interest: The authors declare no conflicts of interest.

References

1. Smalle, J.; Vierstra, R. The ubiquitin 26S proteasome proteolytic pathway. *Annu. Rev. Plant Biol.* **2004**, *55*, 555–590. [PubMed]
2. Pickart, C. Mechanisms underlying ubiquitination. *Annu. Rev. Biochem.* **2001**, *70*, 503–533. [CrossRef] [PubMed]
3. Cho, S.; Ryu, M.; Song, C.; Kwak, J.M.; Kim, W.T. *Arabidopsis* PUB22 and PUB23 are homologous U-box E3 ubiquitin ligases that play combinatory roles in response to drought stress. *Plant Cell* **2008**, *20*, 1899–1914. [CrossRef] [PubMed]
4. Dreher, K.; Callis, J. Ubiquitin, hormones and biotic stress in plants. *Ann. Bot.* **2007**, *99*, 787–822. [CrossRef] [PubMed]
5. Pickart, C.; Eddins, M. Ubiquitin: Structures, functions, mechanisms. *Biochim. Biophys. Acta-Mol. Cell Res.* **2004**, *1695*, 55–72. [CrossRef] [PubMed]
6. Amerik, A.; Hochstrasser, M. Mechanism and function of deubiquitinating enzymes. *Biochim. Biophys. Acta-Mol. Cell Res.* **2004**, *1695*, 189–207. [CrossRef] [PubMed]
7. Verma, R.; Aravind, L.; Oania, R.; McDonald, W.H.; Yates, J.R., III; Koonin, E.V.; Deshaies, R.J. Role of Rpn 11 metalloprotease in deubiquitination and degradation by the 26S proteasome. *Science* **2002**, *298*, 611–615. [CrossRef] [PubMed]
8. Nijman, S.M.B.; Huang, T.T.; Dirac, A.M.G.; Brummelkamp, T.R.; Kerkhoven, R.M.; D'Andrea, A.D.; Bernards, R. The deubiquitinating enzyme USP1 regulates the Fanconi anemia pathway. *Mol. Cell* **2005**, *17*, 331–339. [CrossRef] [PubMed]
9. Nijman, S.M.; Luna-Vargas, M.P.; Velds, A.; Brummelkamp, T.R.; Dirac, A.M.; Sixma, T.K.; Bernards, R. A genomic and functional inventory of deubiquitinating enzymes. *Cell* **2005**, *123*, 773–786. [CrossRef] [PubMed]
10. Varshavsky, A. The ubiquitin system. *Annu. Rev. Biochem.* **1998**, *22*, 383–387.
11. Yan, N.; Doelling, J.; Falbel, T.; Durski, A.; Vierstra, R. The ubiquitin-specific protease family from *Arabidopsis*. AtUBP1 and 2 are required for the resistance to the amino acid analog canavanine. *Plant Physiol.* **2000**, *124*, 1828–1843. [CrossRef] [PubMed]
12. Schwer, H.; Liu, L.Q.; Zhou, L.; Little, M.T.; Pan, Z.; Hetherington, C.J.; Zhang, D.E. Cloning and characterization of a novel human ubiquitin-specific protease, a homologue of Murine UBP43 (Usp18). *Genomics* **2000**, *65*, 44–52. [CrossRef] [PubMed]
13. Amerik, A.; Swaminathan, S.; Krantz, B.; Wilkinson, K.; Hochstrasser, M. In vivo disassembly of free polyubiquitin chains by yeast Ubp14 modulates rates of protein degradation by the proteasome. *EMBO J.* **1997**, *16*, 4826–4838. [CrossRef] [PubMed]
14. Liu, Y.; Wang, F.; Zhang, H.; He, H.; Ma, L.; Deng, X. Functional characterization of the Arabidopsis ubiquitin-specific protease gene family reveals specific role and redundancy of individual members in development. *Plant J.* **2008**, *55*, 844–856. [CrossRef] [PubMed]
15. Wilkinson, K. Regulation of ubiquitin-dependent processes by deubiquitinating enzymes. *FASEB J.* **1997**, *11*, 1245–1256. [CrossRef] [PubMed]
16. Li, Y.; Zheng, L.; Corke, F.; Smith, C.; Bevan, M. Control of final seed and organ size by the DA1 gene family in *Arabidopsis thaliana*. *Genes Dev.* **2008**, *22*, 1331–1336. [CrossRef] [PubMed]
17. Walton, A.; Stes, E.; Cybulski, N.; Bel, M.; Inigo, S.; Durand, A.; Timmerman, E.; Heyman, J.; Pauwels, L.; Veylder, L.; et al. It's time for some "site"-seeing: Novel tools to monitor the ubiquitin landscape in *Arabidopsis thaliana*. *Plant Cell* **2016**, *28*, 6–16. [CrossRef] [PubMed]
18. Nassrallah, A.; Rougée, M.; Bourbousse, C.; Drevensek, S.; Fonseca, S.; Iniesto, E.; Ait-Mohamed, O.; Deton-Cabanillas, A.; Zabulon, G.; Ahmed, I.; et al. DET1-mediated degradation of a SAGA-like deubiquitination module controls H2Bub homeostasis. *eLife* **2018**, *7*, e37892. [CrossRef] [PubMed]
19. Du, L.; Li, N.; Chen, L.; Xu, Y.; Li, Y.; Zhang, Y.; Li, C.; Li, Y. The ubiquitin receptor DA1 regulates seed and organ size by modulating the stability of the ubiquitin-specific protease UBP15/SOD2 in *Arabidopsis*. *Plant Cell* **2014**, *26*, 665–677. [CrossRef] [PubMed]
20. Li, Y.; Xia, T.; Gao, F.; Li, Y. Control of plant branching by the CUC2/CUC3-DA1-UBP15 regulatory module. *Plant Cell* **2020**, *32*, 1919–1932. [CrossRef] [PubMed]
21. Wu, R.; Song, K.; Jing, R.; Du, L. The de-ubiquitinase Ubquitin Specific Protease 15 (UBP15) interacts with the SCF E3 complex adaptor Arabidopsis SKP1 Homologue 1 (ASK1) to regulate petal size and fertility in *Arabidopsis thaliana*. *Plant Sci.* **2024**, *345*, 112112. [CrossRef] [PubMed]
22. Xu, Y.; Jin, W.; Li, N.; Zhang, W.; Liu, C.; Li, C.; Li, Y. Ubiquiitin-specific protease14 interacts with ultraviolet-B insensitive 4 to regulate endoreduplication and cell and organ growth in *Arabidopsis*. *Plant Cell* **2016**, *28*, 1200–1214. [PubMed]
23. Jiang, S.; Wei, J.; Li, N.; Wang, Z.; Zhang, Y.; Xu, R.; Zhou, L.; Huang, X.; Wang, L.; Guo, S.; et al. The UBP14-CDKB1; 1-CDKG2 cascade controls endoreduplication and cell growth in *Arabidopsis*. *Plant Cell* **2022**, *34*, 1308–1325. [CrossRef] [PubMed]
24. Doelling, J.; Yan, N.; Kurepa, J.; Walker, J.; Vierstra, R. The ubiquitin-specific protease UBP14 is essential for early embryo development in *Arabidopsis thaliana*. *Plant J.* **2001**, *27*, 393–405. [CrossRef] [PubMed]
25. Li, W.; Perry, P.; Prafulla, N.; Schmidt, W. Ubiquitin-specific protease 14 (ubp14) is involved in root responses to phosphate deficiency in *Arabidopsis*. *Mol. Plant* **2010**, *3*, 212–223. [CrossRef] [PubMed]

26. Zhao, J.; Zhou, H.; Zhang, M.; Gao, Y.; Li, L.; Gao, Y.; Li, M.; Yang, Y.; Guo, Y.; Li, X. Ubiquitin-specific protease 24 negatively regulates abscisic acid signalling in *Arabidopsis thaliana*. *Plant Cell Environ.* **2016**, *39*, 427–440. [PubMed]
27. Luo, Y.; Takagi, J.; Claus, L.A.N.; Zhang, C.; Yasuda, S.; Hasegawa, Y.; Yamaguchi, J.; Shan, L.; Russinova, E.; Sato, T. Deubiquitinating enzymes UBP12 and UBP13 stabilize the brassinosteroid receptor BRI1. *EMBO Rep.* **2022**, *23*, e53354. [CrossRef] [PubMed]
28. Kong, J.C.; Jin, J.; Dong, Q.; Qiu, J.; Li, Y.; Yang, Y.; Shi, Y.; Si, W.; Gu, L.; Yang, F.; et al. Maize factors ZmUBP15, ZmUBP16 and ZmUBP19 play important roles for plants to tolerance the cadmium stress and salt stress. *Plant Sci.* **2019**, *280*, 77–89. [CrossRef] [PubMed]
29. Zhou, H.; Wang, X.; Huo, C.; Wang, H.; An, Z.; Sun, D.; Liu, J.; Tang, W.; Zhang, B. A quantitative proteomics study of early heat-regulated proteins by two-dimensional difference gel electrophoresis identified OsUBP21 as a negative regulator of heat stress responses in rice. *Proteomics* **2019**, *19*, 1900153. [CrossRef] [PubMed]
30. Zhang, Q.; Zhang, H.; Sun, L.; Fan, G.; Ye, M.; Jiang, L.; Liu, X.; Ma, K.; Shi, C.; Bao, F.; et al. The genetic architecture of floral traits in the woody plant *Prunus mume*. *Nat. Commun.* **2018**, *9*, 1702. [CrossRef] [PubMed]
31. Zhang, Q.; Chen, W.; Sun, L.; Zhao, F.; Huang, B.; Yang, W.; Tao, Y.; Wang, J.; Yuan, Z.; Fan, G.; et al. The genome of *Prunus mume*. *Nat. Commun.* **2012**, *3*, 1318. [CrossRef] [PubMed]
32. Zhao, K.; Zhou, Y.; Ahmad, S.; Yong, X.; Xie, X.; Han, Y.; Li, Y.; Sun, L.; Zhang, Q. PmCBFs synthetically affect PmDAM6 by alternative promoter binding and protein complexes towards the dormancy of bud for *Prunus mume*. *Sci. Rep.* **2018**, *8*, 4527. [CrossRef] [PubMed]
33. Zhang, Y.; Ma, K.; Li, Q. Effects of Low-Temperature Accumulation on Flowering of *Prunus mume*. *Horticulturae* **2023**, *9*, 628. [CrossRef]
34. Dong, B.; Zheng, Z.; Zhong, S.; Ye, Y.; Wang, Y.; Yang, L.; Xiao, Z.; Fang, Q.; Zhao, H. Integrated Transcriptome and Metabolome Analysis of Color Change and Low-Temperature Response during Flowering of *Prunus mume*. *Int. J. Mol. Sci.* **2022**, *23*, 12831. [CrossRef] [PubMed]
35. Yan, L. Pollen Cryopreservation of *Prunus mume*. *J. Beijing For. Univ.* **2004**, *28*, 139–147.
36. Tang, J.; Sun, L.D.; Bao, F.; Han, Y.; Ma, K.; Cheng, T.; Wang, J.; Pan, H.; Zhang, Q. Germplasm resources and breeding of mei, an ornamental woody plant. *Acta Hortic.* **2017**, *1185*, 35–46. [CrossRef]
37. Moon, Y.; Hong, J.; Cho, Y.; Yang, S.; An, G.; Kim, W. Structure and expression of OsUBP6: An ubiquitin-specific protease 6 homolog in rice (*Oryza sativa* L.). *Mol. Cells* **2009**, *28*, 463–472. [CrossRef] [PubMed]
38. Gasteiger, E.; Gattiker, A.; Hoogland, C.; Ivanyi, I.; Appel, R.; Bairoch, A. ExPASy, The proteomics server for in-depth protein knowledge and analysis. *Nucleic Acids Res.* **2003**, *31*, 3784–3788. [CrossRef] [PubMed]
39. Tamura, K.; Stecher, G.; Peterson, D.; Filipski, A.; Kumar, S. MEGA6: Molecular evolutionary genetics analysis version 6.0. *Mol. Biol. Evol.* **2013**, *30*, 2725–2729. [CrossRef] [PubMed]
40. Xie, T.; Chen, C.; Li, C.; Liu, J.; Liu, C.; He, Y. Genome-wide investigation of WRKY gene family in pineapple: Evolution and expression profiles during development and stress. *BMC Genom.* **2018**, *19*, 490. [CrossRef] [PubMed]
41. Hu, B.; Jin, J.; Guo, A.Y.; Zhang, H.; Luo, J.; Gao, G. GSDS2.0: An upgraded gene feature visualization server. *Bioinformatics* **2014**, *31*, 1296–1297. [CrossRef] [PubMed]
42. Bailey, T.; Boden, M.; Buske, F.; Frith, M.; Grant, C.; Clementi, L.; Ren, J.; Li, W.; NobLe, W. MEME SUITE: Tools for motif discovery and searching. *Nucleic Acids Res.* **2009**, *37*, W202–W208. [CrossRef] [PubMed]
43. Liu, R.; Meng, J. MapDraw: A Microsoft Excel macro for drawing genetic linkage maps based on given genetic linkage data. *Hereditas* **2003**, *25*, 317–321. [PubMed]
44. Wang, Y.; Tang, H.; DeBarry, J.; Tan, X.; Li, J.; Wang, X.; Lee, T.; Jin, H.; Marler, B.; Guo, H.; et al. MCScanX: A toolkit for detection and evolutionary analysis of gene synteny and collinearity. *Nucleic Acids Res.* **2012**, *40*, e49. [CrossRef] [PubMed]
45. Liu, C.; Xie, T.; Chen, C.; Luan, A.; Long, J.; Li, C.; Ding, Y.; He, Y. Genome-wide organization and expression profiling of the R2R3-MYB transcription factor family in pineapple (*Ananas comosus*). *BMC Genom.* **2017**, *18*, 503. [CrossRef] [PubMed]
46. Wang, D.; Zhang, Y.; Zhang, Z.; Zhu, J.; Yu, J. KaKs_Calculator 2.0: A toolkit incorporating gamma-series methods and sliding, window strategies. *Genom. Proteom. Bioinform.* **2010**, *8*, 77–80. [CrossRef] [PubMed]
47. Chen, C.; Chen, H.; Zhang, Y.; Thomas, H.R.; Frank, M.H.; He, Y.; Xia, R. TBtools, an integrative toolkit developed for interactive analyses of big biological data. *Mol. Plant* **2020**, *13*, 1194–1202. [CrossRef] [PubMed]
48. Lescot, M.; Déhais, P.; Thijs, G.; Marchal, K.; Moreau, Y.; Van de Peer, Y.; Rouze, P.; Rombauts, S. PlantCARE, a database of plant cis-acting regulatory elements and a portal to tools for in silico analysis of promoter sequences. *Nucleic Acids Res.* **2002**, *30*, 325–327. [CrossRef] [PubMed]
49. Wang, T.; Lu, J.; Xu, Z.; Yang, W.; Wang, J.; Cheng, T.; Zhang, Q. Selection of suitable reference genes for miRNA expression normalization by qRT-PCR during flower development and different genotypes of *Prunus mume*. *Sci. Hortic.* **2014**, *169*, 130–137. [CrossRef]

50. Li, P.; Zheng, T.; Li, L.; Liu, W.; Qiu, L.; Ahmad, S.; Wang, J.; Cheng, T.; Zhang, Q. Integration of chromatin accessibility and gene expression reveals new regulators of cold hardening to enhance freezing tolerance in *Prunus mume*. *J. Exp. Bot.* **2023**, *74*, 2173–2187. [CrossRef] [PubMed]
51. Liu, W.; Liu, H.; Liu, X.; Yue, Z.; Yan, J.; Wei, L.; Wang, H.; Zhao, P.; Bian, G.; Zhang, Q.; et al. Molecular mechanism of cold acclimation regulating freezing tolerance in *Prunus mume*. *Plant Physiol.* **2026**, *201*, kiag333. [CrossRef] [PubMed]
52. Qiao, X.; Li, Q.; Yin, H.; Qi, K.; Li, L.; Wang, R.; Zhang, S.; Paterson, A.H. Gene Duplication and evolution in recurring polyploidization-diploidization cycles in plants. *Genome Biol.* **2019**, *20*, 38. [CrossRef] [PubMed]
53. Holub, E. The arms race is ancient history in *Arabidopsis*, the wildflower. *Nat. Rev. Genet.* **2001**, *2*, 516–527. [CrossRef] [PubMed]
54. Cannon, B.; Mitra, A.; Baumgarten, A.; Young, D.; May, G. The roles of segmental and tandem gene duplication in the evolution of large gene families in *Arabidopsis thaliana*. *BMC Plant Biol.* **2004**, *4*, 10. [CrossRef] [PubMed]
55. Shiu, S.; Karlowski, W.; Pan, R.; Tzeng, Y.; Mayer, K.; Li, W. Comparative analysis of the receptor-like kinase family in *Arabidopsis* and rice. *Plant Cell* **2004**, *16*, 1220–1234. [CrossRef] [PubMed]
56. Doelling, J.; Phillips, A.; Soyler-Ogretim, G.; Wise, J.; Chandler, J.; Callis, J.; Otegui, M.S.; Vierstra, R. The ubiquitin-specific protease subfamily UBP3/UBP4 is essential for pollen development and transmission in *Arabidopsis*. *Plant Physiol.* **2007**, *145*, 801–813. [CrossRef] [PubMed]
57. Cui, X.; Lu, F.; Li, Y.; Xue, Y.; Kang, Y.; Zhang, S.; Qiu, Q.; Cui, X.; Zheng, S.; Liu, B.; et al. Ubiquitin-specific proteases UBP12 and UBP13 act in circadian clock and photoperiodic flowering regulation in *Arabidopsis*. *Plant Physiol.* **2013**, *162*, 897–906. [CrossRef] [PubMed]
58. Wang, D.; Song, W.; Wei, S.; Zheng, Y.; Chen, Z.; Han, J.; Zhang, H.; Luo, J.; Qin, Y.; Xu, Z.; et al. Characterization of the ubiquitin C-terminal hydrolase and ubiquitin-specific protease families in rice (*Oryza sativa*). *Front. Plant Sci.* **2018**, *9*, 1636. [CrossRef] [PubMed]
59. Wu, R.; Shi, Y.; Zhang, Q.; Zheng, W.; Chen, S.; Du, L.; Lu, C. Genome-wide identification and characterization of the ubp gene family in moso bamboo (*Phyllostachys edulis*). *Int. J. Mol. Sci.* **2019**, *20*, 4309. [CrossRef] [PubMed]
60. Song, K.; Zhang, B.; Du, L. Genome-wide identification and analysis of *UBP* gene family in *Quercus robur*. *Trees* **2024**, *38*, 807–821. [CrossRef]
61. Zheng, W.; Du, L. The DUB family in *Populus*: Identification, characterization, evolution and expression patterns. *BMC Genom.* **2021**, *22*, 541. [CrossRef] [PubMed]
62. Gu, Z.; Steinmetz, L.; Gu, X.; Scharfe, C.; Davis, R.W.; Li, W. Role of duplicate genes in genetic robustness against null mutations. *Nature* **2003**, *421*, 63–66. [CrossRef] [PubMed]
63. Ren, R.; Wang, H.; Guo, C.; Zhang, N.; Zeng, L.; Chen, Y.; Ma, H.; Qi, J. Widespread whole genome duplications contribute to genome complexity and species diversity in Angiosperms. *Mol. Plant* **2018**, *11*, 414–428. [CrossRef] [PubMed]
64. Ding, A.; Ding, A.; Li, P.; Wang, J.; Cheng, T.; Bao, F.; Zhang, Q. Genome-wide identification and low-temperature expression analysis of bHLH genes in *Prunus mume*. *Front. Genet.* **2021**, *12*, 762135. [CrossRef] [PubMed]
65. Le, D.; Nishiyama, R.; Watanabe, Y.; Vankova, R.; Tanaka, M.; Seki, M.; Ham, L.H.; Yamaguchi-Shinozaki, K.; Shinozaki, K.; Tran, L.-S.P. Identification and expression analysis of cytokinin metabolic genes in soybean under normal and drought conditions in relation to cytokinin levels. *PLoS ONE* **2012**, *7*, e42411. [CrossRef] [PubMed]
66. Walther, D.; Brunnemann, R.; Selbig, J. The regulatory code for transcriptional response diversity and its relation to genome structural properties in *A. thaliana*. *PLoS Genet.* **2007**, *3*, e11. [CrossRef] [PubMed]
67. Xu, M.; Jin, P.; Liu, T.; Gao, S.; Zhang, T.; Zhang, F.; Han, X.; He, L.; Chen, J.; Yang, J. Genome-wide identification and characterization of UBP gene family in wheat (*Triticum aestivum* L.). *PeerJ* **2021**, *9*, e11594. [CrossRef] [PubMed]
68. Karamat, U.; Tabusam, J.; Khan, M.K.U.; Awan, M.J.A.; Zulfiqar, S.; Du, W.; Farooq, M.A. Genome-Wide Identification, Characterization, and Expression Profiling of Eukaryotic-Specific UBP Family Genes in *Brassica rapa*. *J. Plant Growth Regul.* **2022**, *42*, 3552–3567. [CrossRef]
69. Chang, X.; Wang, T.; Huang, J.; Xu, J.; Ruan, Y.; Liang, Y.; Wang, J. Genome-Wide Identification and Expression Analysis of UBP Genes in Peppers (*Capsicum annuum* L.). *Horticulturae* **2025**, *11*, 458. [CrossRef]
70. Zou, X.; Li, Y.; Yin, H.; Xu, J.; Li, Z.; Jiang, S.; Chen, F.; Li, Y.; Xiao, W.; Liu, S.; et al. Genome-Wide Identification, Characterization, and Expression Analysis under Abiotic Stresses of the UBP Gene Family in Rice (*Oryza sativa* L.). *Agronomy* **2023**, *13*, 2809. [CrossRef]

Disclaimer/Publisher's Note: The statements, opinions and data contained in all publications are solely those of the individual author(s) and contributor(s) and not of MDPI and/or the editor(s). MDPI and/or the editor(s) disclaim responsibility for any injury to people or property resulting from any ideas, methods, instructions or products referred to in the content.